Carbohydrate Polymer Technologies and Applications 9 (2025) 100652

Contents lists available at ScienceDirect

Carbohydrate Polymer Technologies and Applications

journal homepage: www.sciencedirect.com/journal/carbohydrate-polymer-technologies-and-applications

Partially degalactosylated xyloglucan hydrogel artificial niches enhance human spheroids derived from adipose stem cells stemness and differentiation potential

Anna Barbara Di Stefano [a], Emanuela Muscolino [b,c,*], Marco Trapani [a], Francesco Moschella [a], Bartolo Corradino [d], Francesca Toia [a,d], Adriana Cordova [a,d], Clelia Dispenza [b]

[a] BIOPLAST-Laboratory of BIOlogy and Regenerative Medicine-PLASTic Surgery, Dipartimento di Medicina di Precisione in Area Medica, Chirurgica e Critica, Università degli Studi di Palermo, via del Vespro 129, 90127, Palermo, Italy
[b] Dipartimento di Ingegneria, Università degli Studi di Palermo, Viale delle Scienze 6, 90128 Palermo, Italy
[c] Istituto di BioFisica, Consiglio Nazionale delle Ricerche, Via U. La Malfa 153, 90146 Palermo, Italy
[d] Unità di Chirurgia Plastica e Ricostruttiva, Medicina di Precisione in Area Medica, Chirurgica e Critica, Università degli Studi di Palermo, via del Vespro 129, 90127, Palermo, Italy

ARTICLE INFO

Keywords:
Adipose stem cell
3D culture
Hydrogels
Cell encapsulation
Cartilage
Bone
Adipose tissue

ABSTRACT

The role of the hydrogels in cell differentiation and proliferation is critical to the development of tissue engineering and regenerative medicine applications. Understanding the specific mechanisms by which hydrogels interact with cells and how they might influence their behaviour could lead to the design of more effective systems. We analysed the proliferation and mRNAs expression of the spheroids from adipose stem cells (SASCs) mixed to partially degalactosylated xyloglucan (dXG) in a generic culture medium without specific stimulus to assess whether the hydrogel is an “active” or “passive” component in a regenerative context. Overall, our results showed that dXG-based niches with the lowest polymer concentration (1 %w), without recourse to biochemical induction can support cell proliferation and higher commitment toward mesenchymal differentiation.

Hypothesis: Partially degalactosylated xyloglucan hydrogels function as an "active" component in regulating the proliferation and gene expression of adipose stem cell spheroids for regenerative applications.

1. Introduction

Regenerative medicine and tissue engineering are major areas of research with ambitious goals, because they aim to find strategies to regenerate or reconstruct human tissues or entire organs to accelerate natural regeneration processes or overcome the objective difficulty of finding suitable tissue substitutes from compatible donors. In this context, mesenchymal stem cells (MSCs) play a key role due to their ability to self-renew and, under specific stimuli, to differentiate into different tissues such as adipogenic, endothelial, bone and cartilage (Han et al., 2019). MSCs can be harvested either from bone marrow (BM-MSCs) or from adipose tissue (ASCs). The latter site has proven to be more suitable in terms of cell yield and harvesting is certainly less invasive for the patient (Gimble et al., 2007). Spheroids of adipose stem cell (SASCs) represent an interesting source of MSCs for use in basic and translational research and in the clinical field. Indeed, SASCs have a morphology that most closely resembles the physiological condition, maintain stemness over a long period of time, and possess great mesenchymal differentiation capabilities in vitro and in vivo (Di Stefano et al., 2016; Di Stefano, Grisafi, et al., 2021; Di Stefano, Montesano, et al., 2021).

Despite the enormous potential of stem cells, they need a structure that can protect them, keep them at the site of injury and, last but not least, form niches similar to the extracellular matrix present in vivo. For this reason, several scaffolds have been studied that are very promising materials for designing “MSC-friendly niches” (Cosson et al., 2015). They can create an ideal microenvironment for the maintenance of stemness or to stimulate the specific differentiation, increasing the cellular amount. In particular, hydrogels offer the possibility to provide attachment sites for cells and to be loaded with ECM proteins, sugars, and secreted cell factors such as growth factors, immunological factors and metabolic signals that can govern stem cell fate (Ilie et al., 2012).

* Corresponding author.
E-mail address: emanuela.muscolino@unipa.it (E. Muscolino).

https://doi.org/10.1016/j.carpta.2024.100652

Available online 24 December 2024

Xyloglucan (XG) is a structural polysaccharide very common in natural plants, that consists in a highly substituted, non-toxic, easily available and biodegradable material (Chen et al., 2012; Miyazaki, Kawasaki, et al., 2001) and it is FDA approved as food additive (Dea, 1989) and it can be also conveniently tailored by radiation-induced modification of the molecular weight distribution modifying their chemical physical properties for different scopes (Muscolino, Sabatino, et al., 2024). It is composed of a β-(1, 4)-D-glucan backbone chain that is partially substituted by α-(1, 6)-D-xylose, and some of the xylose residues are substituted by β-(1, 2)-D-galactoxylose (Chen et al., 2012; Fry, 1988). A thermally responsive XG variant can be formed using fungal β-galactosidase to remove more than 35 per cent of the galactose residues, becoming partially degalactosylated (dXG) (Brun-Graeppi et al., 2010; Chen et al., 2012). When the galactose removal ratio (GRR) is between 35 % and 50 %, dXG forms gels at body temperature from aqueous solutions of concentration above 1 %w (Shirakawa et al., 1998). Gelation is driven by the association of the more hydrophobic and less branched chain segments. Static and dynamic light scattering studies carried out by de Freitas et al. (De Freitas et al., 2011) suggest that no conformational modification of xyloglucan occurs during degalactosylation and hydrophobic association is the main phenomenon responsible for gel formation. The aggregates formed after degalactosylation behave as rigid rods and act as a crosslinking suture points of the gels, contributing to their solid-like elastic behaviour (Brun-Graeppi et al., 2010). The structure of the network is intrinsically quite heterogeneous, being formed by condensed domains interconnected by association of dangling chains. The higher is the polymer concentration the denser and stronger is the formed network (Todaro, 2014). The porosity is also quite heterogeneous in size, reflecting the heterogeneity of the network. Due to the temperature-responsive behaviour, dXG has already been evaluated as a depot for in situ drug delivery (Kawasaki et al., 1999; Miyazaki et al., 1998; Miyazaki, Kawasaki, et al., 2001; Takahashi et al., 2002) or as a scaffold for soft tissue reconstruction (Dispenza et al., 2017; Nisbet et al., 2006) or mitochondrial transplantation (Picone et al., 2024). Moreover, it has been proposed for the creation of skin patches (Gulino et al., 2024), for oral (Miyazaki, Kawasaki, et al., 2001), ocular (Miyazaki, Suzuki, et al., 2001) and rectal (Miyazaki et al., 1998) drug delivery devices. The in vivo biocompatibility of xyloglucan micellar systems and hydrogels have been demonstrated (Mahajan & Mahajan, 2016; Zhang et al., 2017).

We have evaluated dXG hydrogels as degradable and injectable formulations to deliver SASCs for tissue regeneration (Muscolino, Di Stefano, et al., 2024; Muscolino et al., 2021; Toia et al., 2020). When SASCs were incorporated in an in-situ forming dXG hydrogel, comprising 1 %w of polymer and 50 % v of an in house developed stemness medium (SCM), they showed 100 % viability. Interestingly, when the same hydrogel was formulated by replacing the stemness medium with a medium that stimulates chondrogenic differentiation (CDM) or osteoblastic differentiation (ODM), significant cell proliferation and complete differentiation into chondrocytes or osteoblasts, respectively, was observed after 21 days (Muscolino et al., 2021; Toia et al., 2020).

The fundamental question we asked is whether the dXG hydrogel is an inert (passive) component of the formulation and simply plays a scaffolding role for the cells, or whether it also plays a stimulating (active) role in cell differentiation and proliferation. It is widely recognised that various material characteristics, that can be structural, mechanical, topological, can influence cell fate and their molecular expression genes. Engler et al. (2006) demonstrated that naive mesenchymal stem cells (MSCs) differentiate into certain phenotypes depending on whether the scaffold is elastic or not. Similarly, Seib et al. (2009) studied hydrogels polymerised with gelatine and thiol-modified hyaluronic acid demonstrating that the vascular epithelial growth factor (VEGF) and interleukin-8 (IL8) expression were higher when cells were cultured on hard substrates compared to soft ones. Joon Kwon (2013) demonstrated that the chondrogenesis from mesenchymal stem cells on sulfonate-coated polyacrylamide gels (S-PAAm gels) is regulated by their stiffness. In particular, gene investigations on mRNA expression levels showed an increase of collagen, type II, alpha (Col2a1), aggrecan (Agc) and SRY-Box Transcription Factor 9 (Sox9) in MSCs grown on low-stiffness gels (22-fold, 8-fold and 3-fold, respectively), compared to undifferentiated MSCs on polystyrene plate (PS), and decreased in direct proportion to the increase in gel stiffness. Our study diverges from these works and our previous works (Muscolino, Di Stefano, et al., 2024; Muscolino et al., 2021; Toia et al., 2020) by examining the influence of degalactosylated xyloglucan (dXG) hydrogels on stem cell fate in a simple growth medium (DMEM) devoid of biochemical differentiation cues. Moreover, by systematically varying polymer concentration, we uncovered the contribution of hydrogel porosity and mechanical properties to cell proliferation and differentiation without external biological stimuli. In order to clarify the role of dXG in the fate of SASCs, dXG-based niches with various porosity and mechanical properties were obtained by using three concentrations of polymer (1 %w, 1.5 %w and 2.5 %w). They were formulated with SCM and DMEM. While the polymer concentration increases, the concentration of the various solutes coming from the culture media decrease. Polymer concentration as well as the concentration of other solutes have an impact on the network structure and hence on the mechanical properties and porosity of the hydrogel niches. Cell proliferation and gene expression levels of several markers related to stemness or differentiation towards the major mesenchymal lineages were measured and discussed.

2. Experimental

2.1. Materials

Tamarind seeds xyloglucan was purchased from Megazyme International (Ireland). Sugar composition of the tamarind seed xyloglucan is xylose 34 %w; glucose 45 %w; galactose 17 %w; arabinose and other sugars 4 %w, as provided by Megazyme International. β-Galactosidase from Aspergillus oryzae (11.8 U/mg) was purchased from Sigma Chemicals (USA). Tamarind seeds xyloglucan was degalactosylated according to an established protocol, to obtain a degalactosylation degree of ca. 45 % (Brun-Graeppi et al., 2010; Shirakawa et al., 1998).

2.2. Cell culture

Adipose tissue samples were obtained from healthy subjects by liposuction in different parts of the body, after approval of an informed consent. The patients recruited in the study were twelve, 4 males and 8 females, with a mean age of 50 years with a range between 42 and 64 years. Then, the lipoaspirates were digested, first mechanically (30 min at 37 °C under agitation) and then enzymatically (collagenase 150 mg/ml, Gibco, Carlsbad, CA). After digestion, samples were centrifuged at 1200 rpm for 5 min forming the stromal vascular fraction (SVF) which was recovered and resuspended in stem cell condition. After isolation, the spheroids were plated in a mixture of DMEM and fetal bovine serum (FBS) (EUS00KP, euroclone) and maintained at 37 °C in a humidified 5 % CO_2 incubator for 7, 14, and 21 days.

2.3. Hydrogel preparation

Weighed amounts of dXG were dissolved in 0.22 um cut-off prefiltered, distilled water to obtain 2 %w, 3 %w and 5 %w polymer concentration dispersions, by stirring for about 2 h at 5 °C. The dispersions were autoclaved at 120 °C for 20 min and then stored at 4 °C. Known volumes of the aqueous polymeric dispersions obtained were gently mixed with the same volume of water, SCM, DMEM culture medium, i.e. in a 1:1 vol ratio, and incubated at 37 °C for 10 min before any further use. Each system is referred as dXGx-z, where x is a number that represent the final polymer concentration, z is a letter referring to water (W), SCM (S) or DMEM (D). The composition of each system is

schematized in Table 1.

These systems will be collectively identified as T0. The systems after 7 days, 14 days and 21 days incubation at 37 °C are identified with the codes T7, T14 and T21, respectively.

2.4. Cell loading, incubation, and SASCs recovery

Cells were loaded onto dXG systems by mixing dXG dispersions with the same volume of SASC-3D dispersions in SCM or in DMEM, within 96-well multiwells. In all cases, 50,000 cells/well were loaded and maintained in a CO_2 incubator at 37 °C for 21 days. Cell proliferation was monitored under a light microscope (Leica DM IL LED Fluo). Cell recovery from the hydrogels was performed by incubation with an aqueous solution of Cellulase from Trichoderma reesei (Sigma Aldrich) at a final concentration of 84 U/ml for 90 min at 37 °C. Subsequently, centrifugation at 1200 RPM for 5 minu at 4 °C, and removal of supernatant dispersion was performed.

2.5. Rheological analysis

Rheological analysis under small-oscillatory conditions was performed using a stress-controlled AR G2 rheometer (TA Instruments) with a 20-mm PIK non-slip plate. Amplitude-sweep measurements were performed to identify strain values for which the materials are within the linear elastic range, at 1 Hz. Constant strain frequency sweep measurements were performed at a constant strain, in the range of 4×10^{-4} to 1×10^{-2} depending on the system, and the frequency was varied between 0.1 Hz and 10 Hz. Known volumes of formulations were placed on the bottom plate of the rheometer and measurements began after 10 min of thermal and structural equilibration at the measurement temperature of 37.0 ± 0.1 °C, controlled by an embedded Peltier system. The represented graphs of storage modulus, G', and loss modulus, G", are the arithmetic mean of three curves obtained by measurements carried out with samples from different preparation batches.

The flow curves of the dispersions formulated with SCM and DMEM were obtained operating the rheometer in rotational mode at the constant temperature of 25.0 ± 0.1 °C, the temperature of the intended injection. Measurements were performed with the PIK anti-slippery of 20 mm diameter and a gap of 1000 μm, varying the shear rate between 0.1 and 100 1/s.

Creep-recovery tests were performed by imposing for every system a stress equal to 30 % of the stress corresponding to strain linearity limit, observed through amplitude-sweep tests, with a 20-mm PIK non-slip plate at the constant temperature of 37.0 ± 0.1 °C, for 50 s for creep phase and 360 s for recovery phase.

In the creep-recovery tests, the total strain at the end of creep phase can be split in a recoverable part, γ_e (related to material elasticity), and a non-recoverable part, γ_v (related to material viscosity).

The recovery ratio percentage, evaluated at final time of interest for tests, is here defined as the percentage ratio between the total recoverable strain and the total strain and it was used to plot the results:

Recovery ratio percentage $= \gamma_e/(\gamma_e + \gamma_v)\%$

Stress relaxation tests were performed by imposing for every system a strain equal to 30 % of the strain linearity limit, observed though amplitude-sweep tests, with a 20-mm PIK non-slip plate at the constant temperature of 37.0 ± 0.1 °C, for 360 s.

The stress relaxation decay percentage is defined as follows and it was used to plot the results:

Relaxation decay percentage $= (Gt_0 - Gt_1)/Gt_0\%$

Where Gt_0 is the initial stress relaxation modulus, read after 0.02 s, and Gt_1 is the stress relaxation modulus read after 20 s, a significative time instant of the stress-relaxation test.

2.6. Scanning electron microscopy (SEM)

Hydrogel morphology was investigated using a Field Emission Scanning Electron Microscope (SEM) Phenom ProX desktop at 10kV of accelerating voltage. Hydrogel samples were frozen in liquid nitrogen, freeze-dried, gold coated by JFC-1300 gold coater (JEOL) on aluminium stabs just before scanning.

2.7. Cell viability analysis

Cell viability of SASCs under all conditions was quantified using the MTS assay (3-(4,5-dimethylthiazol-2-yl)-5-(3-carboxymethoxyphenyl)-2-(4-sulfophenyl)-2H tetrazolium) assay (Promega). Cells were incubated in a 96 multi-well at a density of 50,000 cells/well at a 1:1 ratio with the different scaffold concentrations and embedded 100 μl of SCM/DMEM every 3 days. The absorbance at 490 nm was analysed at 7, 14 and 21 days of incubation using the TECAN spectrophotometer Spark 10 M

2.8. mRNA expression profile

Total RNA was extracted from cells recovered from the hydrogels after 14 days of incubation with DMEM, using RNeasy Mini Kit (Qiagen). Qubit4 fluorometer (Invitrogen) was used for quantification, and RNA (175 ng) was retrotranscribed into cDNA via the High-Capacity cDNA Reverse Transcription Kit (Applied Biosystems). The different conditions were all performed in triplicate and the primers used were multiple for the different differentiation fates. the Taqman primers (Thermo Fisher) were: SOX2 (Hs01053049_s1), NANOG (Hs04399610_g1) and POU5F1 (Hs00999632_g1) as stemness markers; RUNX2 (Hs00231692_m1) and ALP (Hs01029144_m1) as osteoblastic markers; SOX9 (Hs01001343_g1) and Col10A1 (Hs00166657_m1) as chondroblastic markers and finally PPARγ (Hs01115513_g1) and LPL (Hs00173425_m1) as adipocyte markers. GAPDH (Hs02758991_g1) was employed as a housekeeping gene. The relative expression mRNA levels were calculated using the 2-ΔΔCt Livak method.

2.9. Statistical analysis

Data are expressed as mean ± standard deviation (SD) of three independent experiments conducted in triplicate. Statistical significance

Table 1
Final composition of the hydrogels.

Code	dXG, %w	Water, % w	Medium, %v	Salts (g/l)	Glucose (g/l)	Aminoacids (g/l)
dXG1-W	1	99	\	\	\	\
dXG1-S	1	49	50	3.466	2.465	0.837
dXG1-D	1	49	50	10.100	4.500	5.570
dXG1.5-W	1.5	98.5	\	\	\	\
dXG1.5-S	1.5	48.5	50	3.466	2.465	0.837
dXG1.5-D	1.5	48.5	50	10.100	4.500	5.570
dXG2.5-W	2.5	97.5	\	\	\	\
dXG2.5-S	2.5	47.5	50	3.466	2.465	0.837
dXG2.5-D	2.5	47.5	50	10.100	4.500	5.570

was observed using the One Way Anova test, followed by Bonferroni's multiple comparison test. Significance levels are indicated as p values: * $p < 0{,}001$.

3. Results

3.1. Mechanical and morphological properties of the hydrogel niches

Most biological tissues, and the extracellular matrix among them, are viscoelastic materials. For this reason, the mechanical characterisation of the artificial niche has been performed by applying a dynamic, small amplitude oscillatory shear to determine the elastic component (G', storage modulus) and the viscous component (G", loss modulus) of the complex modulus as function of the oscillation frequency. The matrix creep, i.e. its ability to deform with time, as well as its stiffness, play important roles in the growth and differentiation of specific cell types from MSCs (Cameron et al., 2014, 2011). G' and G" curves for the hydrogels as produced, formulated either with SCM or DMEM, are reported in Fig. 1. In particular, Fig. 1**A** shows the rheological behaviour of the hydrogels with 1 %w, 1.5 %w and 2.5 %w dXG, formulated with SCM, and Fig. 1**B** the G' and G" curves of the corresponding systems formulated with DMEM. The rheological behaviour of the systems with SCM have been already described in previous papers (Muscolino, Di Stefano, et al., 2024; Toia et al., 2020) and their G' and G" curves are included here for comparison. dXG1-S behaves as a weak gel with a heterogeneous network structure: the G" curve is lower than the G' curve at low frequencies and approaches G' at higher frequencies; the marked frequency dependence of both curves suggests a wide range of relaxation times. By increasing the polymer concentration to 1.5 %w, in dXG1.5-S, G' becomes an order of magnitude higher than G", that is characteristic of relatively strong hydrogels, and G' and G" curves become independent of frequency, a sign of a more homogeneous network structure. Interestingly, by further increasing the polymer concentration, in dXG2.5-S, the frequency dependence returns, albeit at low frequencies; the values of G' increase to almost 2 kPa and the separation between the G' and G" curves is greater. To evaluate the possible injectability of the dXG hydrogels, rheological measurements were performed to determine viscosity as a function of shear stress (Fig. 1**C**). All formulations demonstrated pronounced shear-thinning behavior, indicative of excellent injectability. This characteristic ensures that the hydrogels can maintain their structural integrity under low-stress conditions while enabling smooth flow through syringe needles during high-stress scenarios. This property is particularly beneficial for minimally invasive delivery methods in tissue engineering and regenerative medicine applications.

We can conclude that dXG2.5-S is the strongest hydrogel among the three, but the physical network has not yet fully developed, probably due to slower dynamics caused by the increased viscosity at higher polymer concentration.

As already observed elsewhere, the composition of the swelling

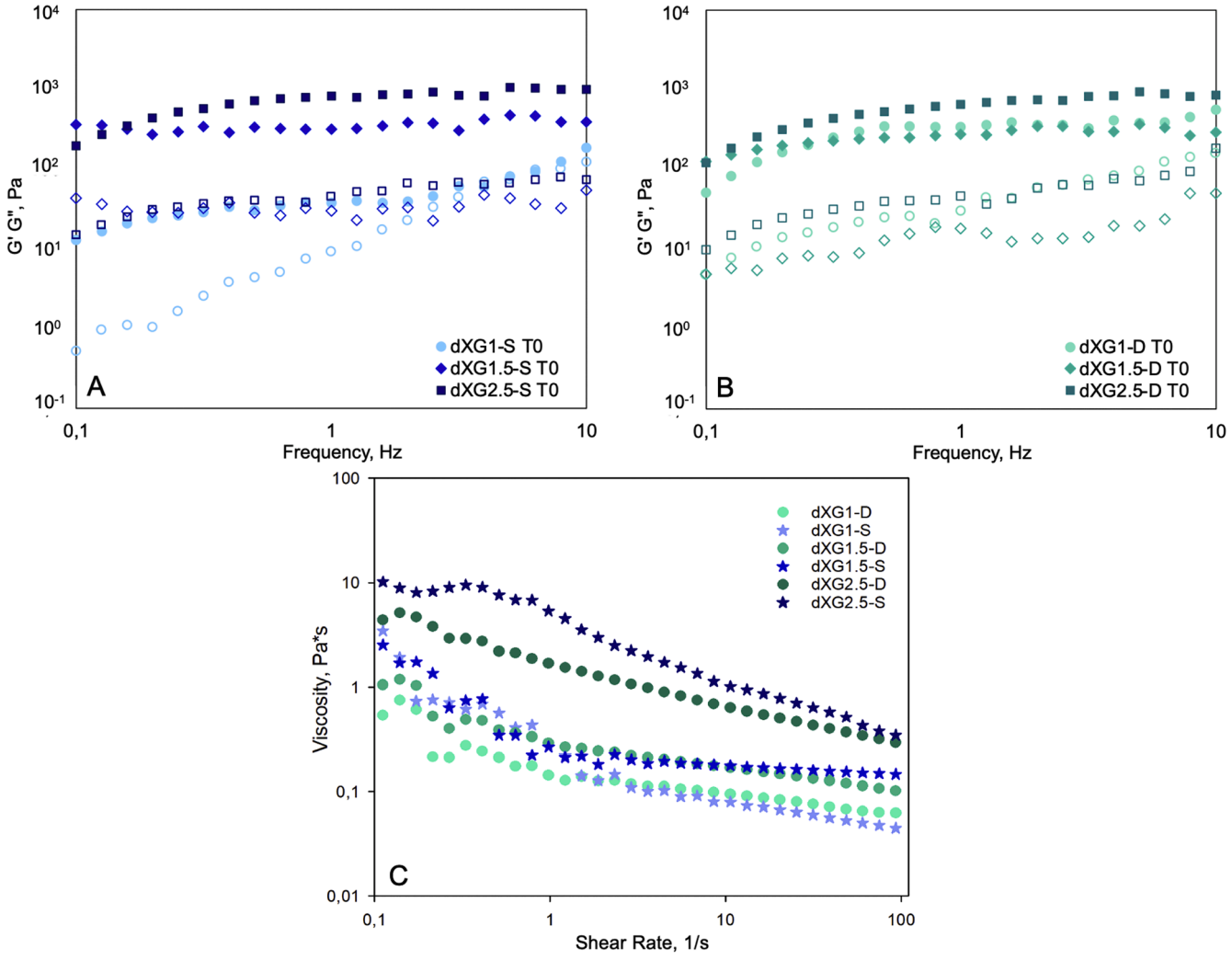

Fig. 1. Storage modulus, G' (full dot), and loss modulus, G" (hollow dot) as function of frequency of dXG1, dXG1.5 and dXG2.5 hydrogels conditioned with SCM (A) and DMEM (B) at T0 and 37 °C, Shear viscosity of dXG1, dXG1.5 and dXG2.5 dispersions mixed with SCM or DMEM (C) as a function of the shear rate at 25 °C.

medium has an effect on the hydrogel structure due to the physical nature of the crosslinking points (Muscolino et al., 2021). dXG1-D (see Fig. 1**B**) has the highest values of G' and G" among all systems, the curves are only frequency-dependent at low frequency, and G' is always almost an order of magnitude higher than G". This hydrogel has the highest elastic modulus, but also the highest capacity to dissipate energy through relaxation. DMEM has a higher concentration of salts and proteins than SCM, and their amount relative to the polymer, is the highest for dXG1. The influence of the nature of the medium on the viscoelastic behavior of hydrogels is much less evident as the polymer concentration increases.

The evolution of the structure during the incubation at 37 °C was investigated by rheological analysis after 7 days (T7), 14 days (T14) and 21 days (T21). The mechanical spectra are reported in Fig. 2**A–F**, while the average G' and G" values in the whole frequency range are reported in Fig. 2**G–I**. In general, the incubation at 37 °C produces an attenuation to full disappearance of the frequency dependency in the systems that had initially exhibited it. The systems at 1 %w have more distinctive trends because they are more affected by the composition of the culture medium, while for the hydrogels at higher polymer concentrations the evolution of the mechanical properties in time is less affected by the nature of the medium. In general, there is a slight decrease in G' with an increase in G", during the first 7–14 days, when we expect the networks to equilibrate with the medium at 37 °C, followed by an increase in both G' and G'' because of a structural reorganization of the network.

Creep-recovery and stress-relaxation tests were performed for the systems from T0 to T14 (time of the most interest for our study) and for the system with SASCs and DMEM at T14 also, to elucidate the viscoelastic properties of the hydrogels, particularly focusing on their time-dependent deformation and recovery. The Recovery ratio percentage, calculated from creep-recovery tests, and the Relaxation decay percentage, calculated from stress-relaxation tests, provide critical insights into how the hydrogels behave under mechanical stress, making them relevant for applications where cells interact dynamically with the matrix and the results are presented in Fig. 3.

From the presented data, it is evident that both relaxation decay and recovery ratio percentages are generally high across the studied systems, although with some variability depending on dXG concentration, culture media, and time points. This observation suggests that these systems possess a unique combination of elastic recovery and stress relaxation characteristics.

A plausible explanation for these mechanical behaviors lies in the microstructure of the hydrogels. As previously observed (Dispenza et al., 2020) dXG hydrogels are composed of dense, well-formed crosslinking zones or clusters that provide a robust elastic response, allowing the system to partially recover after deformation (as reflected in the recovery ratio). These dense areas are interconnected by more loosely crosslinked or amorphous regions, which are responsible for the system ability to relax stress over time (as seen in the high relaxation decay values). This microstructural arrangement resembles a composite material, where rigid "marble-like" elements are embedded in and interconnected by a softer, more flexible matrix.

Such a structure would inherently allow for both a quick initial elastic recovery and a subsequent stress dissipation, as the softer regions undergo relaxation under sustained deformation. The balance between these two behaviors may be modulated by factors such as polymer concentration and environmental conditions (e.g., media type or the presence of cells).

Due to the heterogenous nature of the systems it is difficult to find a trend, but some observation can be made. For instance, higher dXG

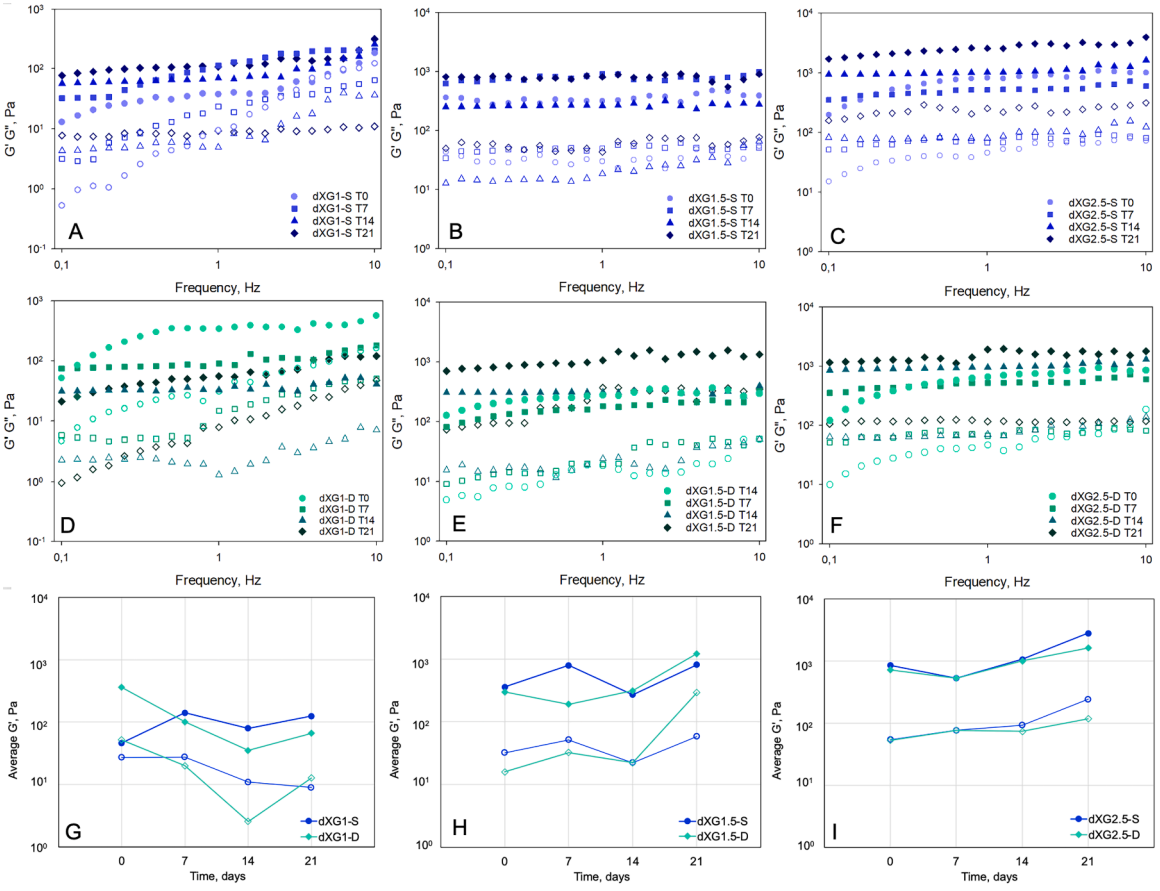

Fig. 2. Storage and loss moduli as function of oscillatory frequency of the hydrogels as prepared (T0) and after 14 days (T14) and 21 days (T21) of incubation. (A) 1 %w dXG with SCM; (B) 1.5 %w dXG with SMC; (C) 2 %w dXG with SCM; (D) 1 %w dXG with DMEM; (E) 1.5 %w dXG with DMEM; (F) 2 %w dXG with DMEM.

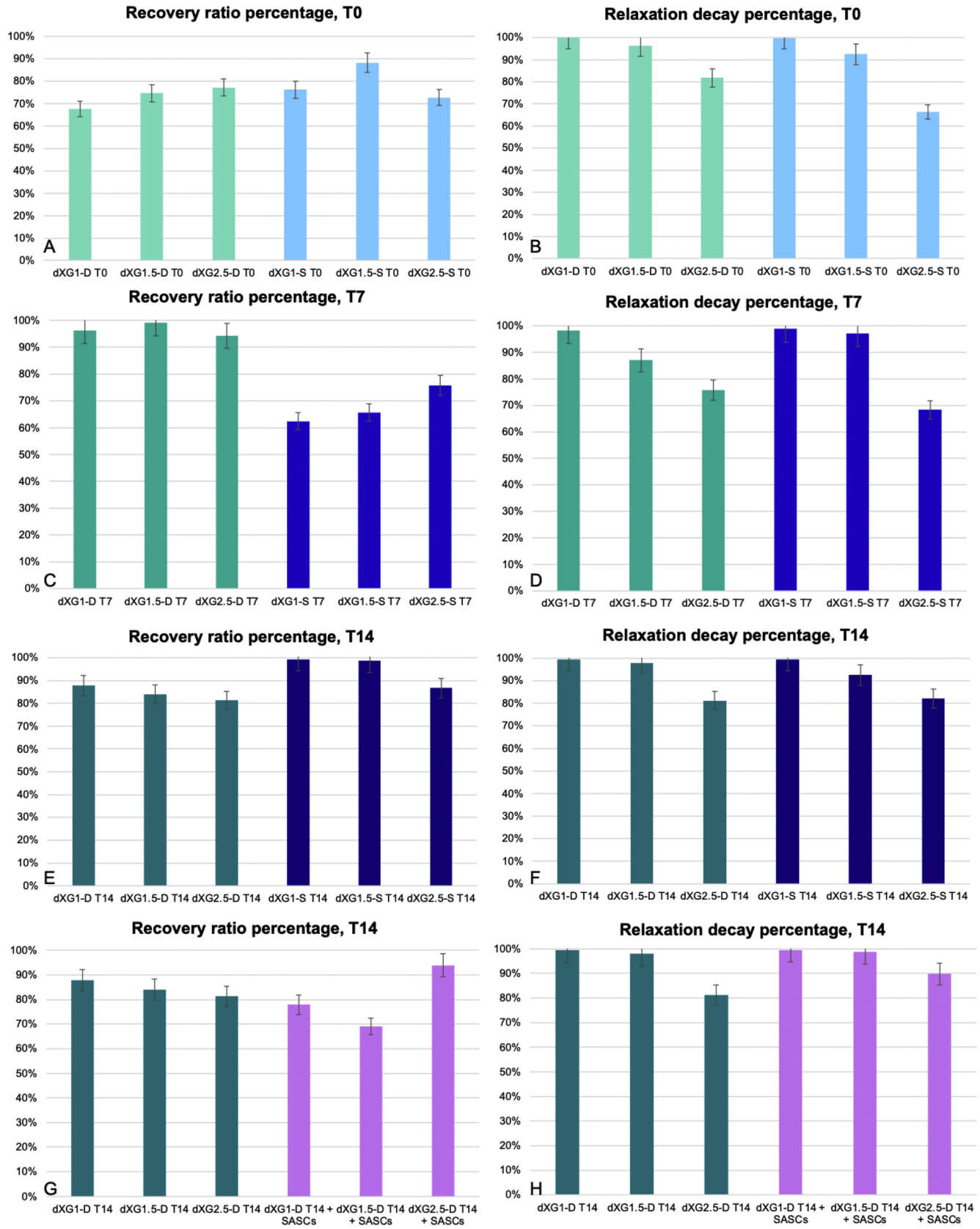

Fig. 3. Recovery ratio percentages of dXG hydrogels conditioned with SCM and DMEM, at T0 (A), T7 (C) and T14 (E) and comparison between dXG hydrogels conditioned with DMEM at T14 with and without SASCs (G). Relaxation decay percentages of dXG hydrogels conditioned with SCM and DMEM, at T0 (B), T7 (D) and T14 (F) and comparison between dXG hydrogels conditioned with DMEM at T14 with and without SASCs (H).

concentrations (e.g., dXG2.5) generally lead to greater crosslink density, resulting in lower relaxation decay and in some cases an improved recovery ratio. Lower concentrations (e.g., dXG1) likely have fewer crosslinking points and more amorphous regions, which could enhance relaxation but may compromise recovery ratio. Media type and the presence of cells appear to introduce additional variability, possibly due to interactions between the hydrogel matrix and surrounding biological components, which could alter the effective crosslinking or hydration state of the network.

Overall, this combination of dense and loose crosslinking regions gives rise to the observed mechanical behavior, making these hydrogels adaptable to different functional demands. In the context of applications, these properties might be advantageous for balancing the need for elasticity with the ability to dissipate stresses during dynamic loading conditions. Furthermore fast stress relaxation can greatly enhance cell migration and proliferation (Bertsch et al., 2022).

When it comes to observe how SASCs possibly influence the mechanical properties in the dXG1-D T14 system, there is little to no difference in relaxation decay with and without cells, with values of 99.48 % and 99.57 %, respectively. This suggests that the presence of cells does not significantly alter the hydrogel's stress-relaxation behavior at this low concentration. A similar pattern is observed in the dXG1.5-D T14 system, where the relaxation decay increases slightly from 97.95 % without cells to 98.65 % with cells. This change indicates that cellular activity may have a subtle impact, potentially enhancing the hydrogel's ability to dissipate stress. In the dXG2.5-D T14 system, however, the relaxation decay significantly increases from 81.15 % without cells to 89.78 % with cells, pointing to a more pronounced effect of cell presence. This increase suggests that the denser matrix in the higher concentration hydrogel interacts more dynamically with the cells, possibly due to cellular remodeling or alterations in crosslinking dynamics.

The recovery ratio shows a more pronounced trend with the inclusion of cells. In the low-concentration hydrogels (dXG1-D and dXG1.5-D), the recovery ratio decreases when cells are present, from 87.82 % to 77.91 % in dXG1-D T14 and from 84.00 % to 69.11 % in dXG1.5-D T14. This suggests that cell activity, which may involve matrix remodeling, interferes with the hydrogel ability to recover elastically, particularly at lower concentrations. In contrast, for dXG2.5-D T14, the recovery ratio increases with cells, from 81.25 % without cells to 93.90 % with cells. This increase indicates that at higher concentrations, the hydrogel matrix may provide better support for cellular activity, improving both stress-relaxation and recovery behavior.

The morphology of the hydrogels after quenching in liquid nitrogen and freeze-drying was investigated by SEM (Fig. 4). All systems mixed with the culture media underwent volume contractions after lyophilisation, the more significant the lower was the polymer concentration. This prevents a meaningful determination of pore size. Still some interesting observations can be made from the comparison among the systems. DMEM favours the formation of a fibrous network with an open and interconnected porosity. On the contrary, SCM favors dXG assembly in thin membranes. In agreement with the rheology data, the differences between the systems formulated with the two media are attenuated at the increase of polymer concentration. In Fig. 5, we compare the SEM morphologies of dXG1.5 and dXG2.5 systems formulated with SCM and DMEM, with the corresponding ones for the systems formulated with CDM and ODM (Muscolino et al., 2021) after 21 days of incubation at 37 °C. We clearly see similarities between dXG1.5-D and dXG1.5-C and among all the dX2.5 systems. These last hydrogels will be artificial niches for SASCs-3D with the same chemical structure of the polymeric scaffold, similar viscoelastic properties and morphology, but nominally different ability to provide specific biochemical cues to the stem cells, thanks to the different composition of the swelling/incubation media.

3.2. Cell viability of SASc-3D in dXG hydrogel niches

A quantitative analysis of cell viability of free SASCs-3D, i.e. fluctuating within low adhesion flasks in SCM, and of SASCs embedded in the various hydrogels formulated with either SCM or DMEM was performed through MTS assay (Fig. 6 **A and B**). The viability of the systems with SCM have been already described in previous papers (Muscolino, Di Stefano, et al., 2024; Toia et al., 2020) and it is included here for comparison. SASCs in SCM are usually quiescent, characterized by very low clonogenicity (Di Stefano et al., 2016). When they are incorporated in dXG hydrogels formulated with SCM (Fig. 6**A**), we observe maintenance of cell viability for dXG1-S at T7 and a decrease in viability for dXG1.5-S and dXG2.5-S. From T7 to T14 we witness a significant proliferation, both in dXG1-S (4-fold) and in dXG 2.5-S (5-fold). Even in dXG1.5-S, where at T7 the residual viability was very low, there is partial recovery. Compared to T14, T21 evidences a reduction in viability. When hydrogels are formulated with DMEM (Fig. 6**B**), there is no significant mortality at T7 and always an increase of viability at T14; 12-fold in dXG1-D, 4-fold in both dXG1.5-D and dXG2.5-D. Also in these cases, the viability decreases at T21. In addition to the MTS analysis, we collected morphological evidence of cell distribution in hydrogels with DMEM, at different concentrations and times (Fig. 6**C**). In the case of dXG1-D, the cells spread and colonised the scaffold (it was possible to see a uniform distribution of cells at different depths). Overcrowding, in other words the lack of space and nutrients to support the significant expansion experienced in the first 14 days, is a possible explanation for why the systems show mortality after 14 days. In densely cross-linked scaffolds, with more dense and rigid regions, such as dXG1.5-D and dXG2.5-D, overcrowding may be local and thus already achieved with a lower total number of cells.

In Fig. 7**A–C**, we compare the cell viability results obtained incorporating SASCs in dXG1 (Fig. 7**A**), dXG1.5 (Fig. 7**B**) and dXG2.5 (Fig. 7**C**) hydrogels formulated with the four media SCM, DMEM, ODM or CDM. Data for ODM and CDM are from Muscolino et al. (Muscolino et al., 2021). For dXG1 systems the highest viability is for DMEM at T14 and is only similar to the one measured for dXG1-C at T21, when the stem cells were differentiated in chondrocytes. Also, for dXG1.5 systems, DMEM and CDM are the media that favour most proliferation, although viability values are lower than those obtained for dXG1. Contrarywise,

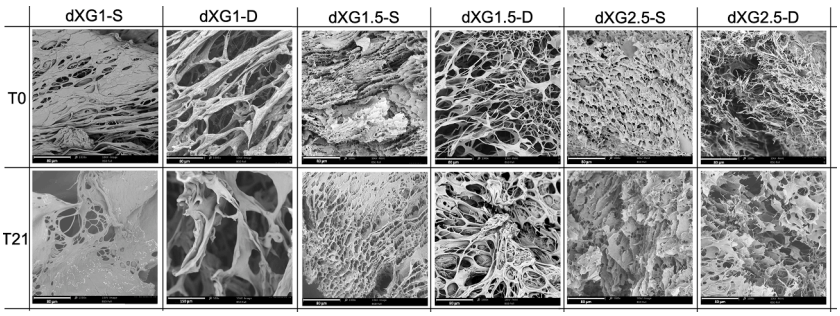

Fig. 4. SEM micrographs (cross-sections) of dXG hydrogels conditioned with SCM and DMEM, at T0 and T21 (scale bar 80 um). For dXG1-D T21 the scale bar is 150 μm. (dXG1-S and dXG2.5-S systems are inserted for completeness and comparison (Muscolino, Di Stefano, et al., 2024)).

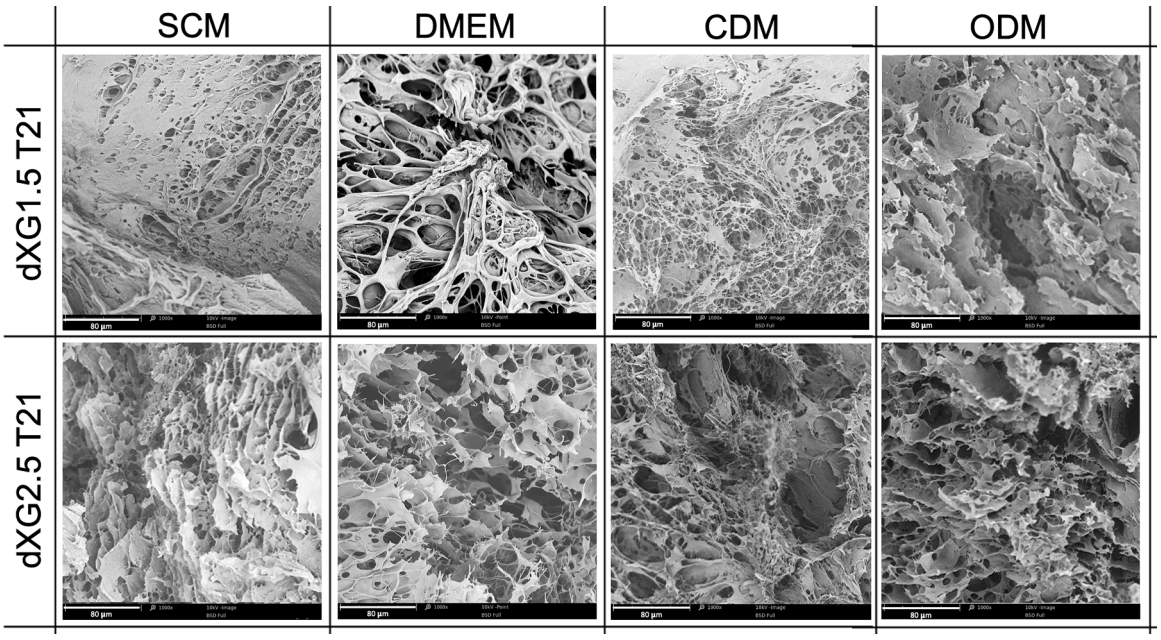

Fig. 5. SEM micrographs (cross-sections) of dXG1.5 and dXG2.5 hydrogels conditioned with SCM, DMEM, CDM and ODM at T21 (scale bar 80 um) (Muscolino et al., 2021).

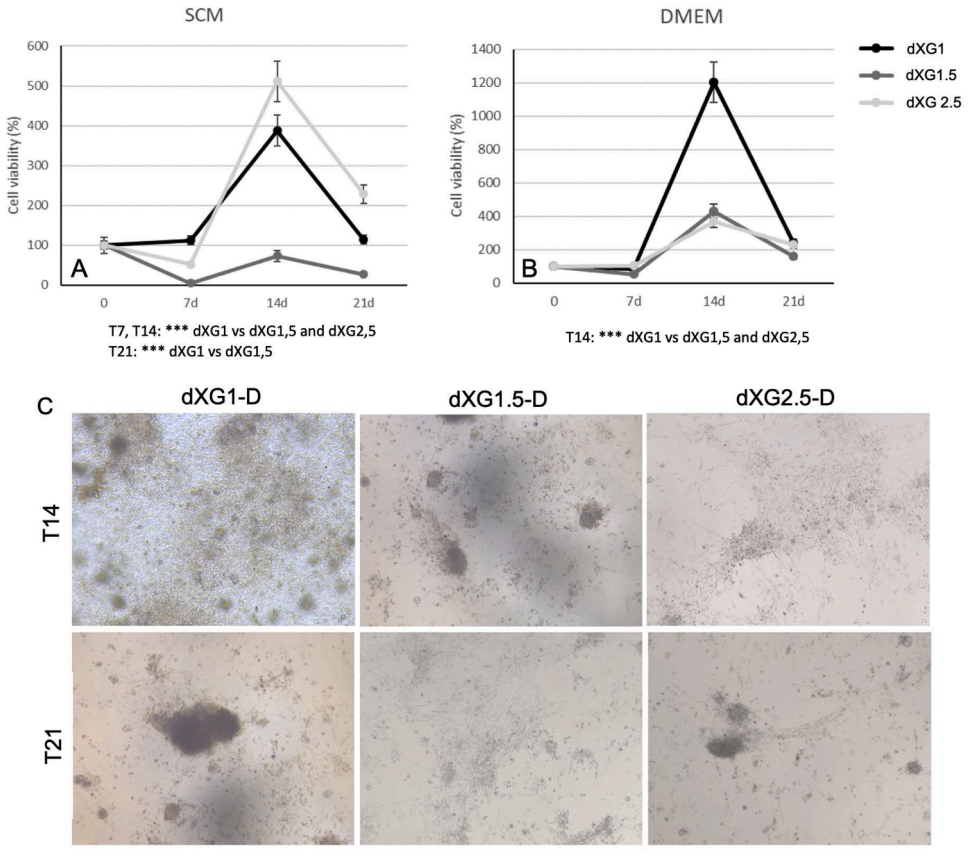

Fig. 6. Cell viability of SASCs incorporated in dXG hydrogels in SCM (A) and in DMEM (B) (dXG1-S and dXG2.5-S systems are inserted for completeness and comparison (Muscolino, Di Stefano, et al., 2024); Optical microscope images of dXG1-D, dXG1.5-D, dXG2.5-D systems at T14 and T21 (C).

dXG2.5 hydrogels at 14 days show the highest viability values for SASCs-3D when formulated and incubated with SCM.

3.3. Gene expression of SASc-3D in dXG hydrogel niches

To understand whether the increase in cell viability observed in DMEM-formulated dXG systems could be attributed to some kind of

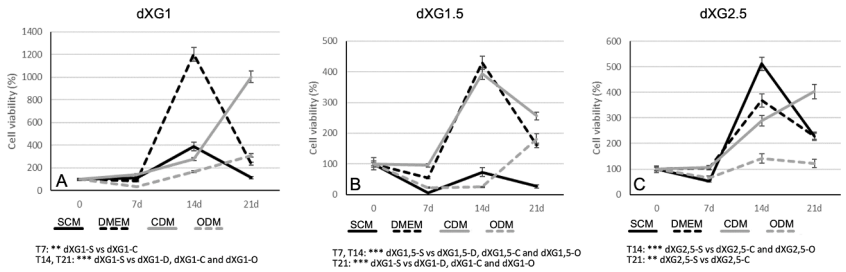

Fig. 7. Comparison of cell viability of SASCs in SCM, DMEM, CDM and ODM incorporated in dXG-1 (A), in dXG-1.5 (B) and in dXG-2.5 (C) hydrogels (Muscolino et al., 2021).

differentiation stimulus that stem cells receive directly from the dXG scaffold, an investigation of mRNAs coding for several genes was conducted. Specifically, three stemness-associated genes (SOX2, NANOG, and POUF51), two osteoblastic genes (RUNX2 and ALP), two chondrogenic genes (SOX9 and COL10A1) and two adipocyte genes (PPAR-γ and LPL) were searched in SASCs-3D incubated in the three DMEM-formulated dXG hydrogels, after 14 days of incubation with the same medium. The same genes were searched in the scaffold free-SASCs-3D incubated in SCM and used as reference.

Analysis of stemness genes shows that SASCs-3Ds in dXG1-D have a 35-fold increase in SOX2, 30-fold increase in NANOG and 15-fold increase in POUF51 compared with SASCs-3Ds without scaffolds incubated in SCM. For dXG1.5-S SASCs-3Ds, there is a 10-fold increase in SOX2, 5-fold increase in NANOG and 2-fold increase in POUF51. In dXG2.5-S, there is an almost 5-fold increase in SOX2, 3-fold increase in NANOG and the same amount of POUF51 (Fig. 8**A**).

The analysis of osteoblastic genes showed that in all systems there is an upregulation of RUNX2, a transcription factor that is expressed in early osteoblast-lineage cells, in comparison to fluctuating SASCs-3D in SCM, but also in comparison to terminally differentiated osteoblasts from scaffold free-SASCs-3D. Specifically, the increase of RUNX2 was 12-fold, 5-fold and 10-fold, for dXG1-D, dXG1.5-D and dXG2.5-D, respectively. The expression of RUNX2 in SASCs incorporated in the same hydrogels but formulated and incubated for 21 days with the osteogenic differentiation medium, ODM, was ~120-fold, ~50-fold and ~10-fold, respectively (Muscolino et al., 2021). Contrarywise, ALP expression – an enzyme involved in the late osteoblastic differentiation – was upregulated only in the dXG1 (7-fold) and significantly more upregulated (36-fold) in differentiated osteoblasts from scaffold free-SASCs-3D (Fig. 8**B**).

The study of chondrocyte genes was conducted with SOX 9 and COL10A1, as in our previous study with SASCs-3D in CDM-formulated dXG hydrogels (Muscolino et al., 2021). SOX9 is a key transcription factor in cartilage development. COL10A1 is a marker of hypertrophic mature chondrocytes, a final stage of chondrocyte differentiation. Regarding SOX9 mRNA, the best niche is dXG1-D with an approximately 17-fold increase in SOX9 compared with scaffold free-SASCs-3D in SCM. SOX9 was also upregulated in dXG1.5 (5-fold) and dXG2.5 (10-fold). It is

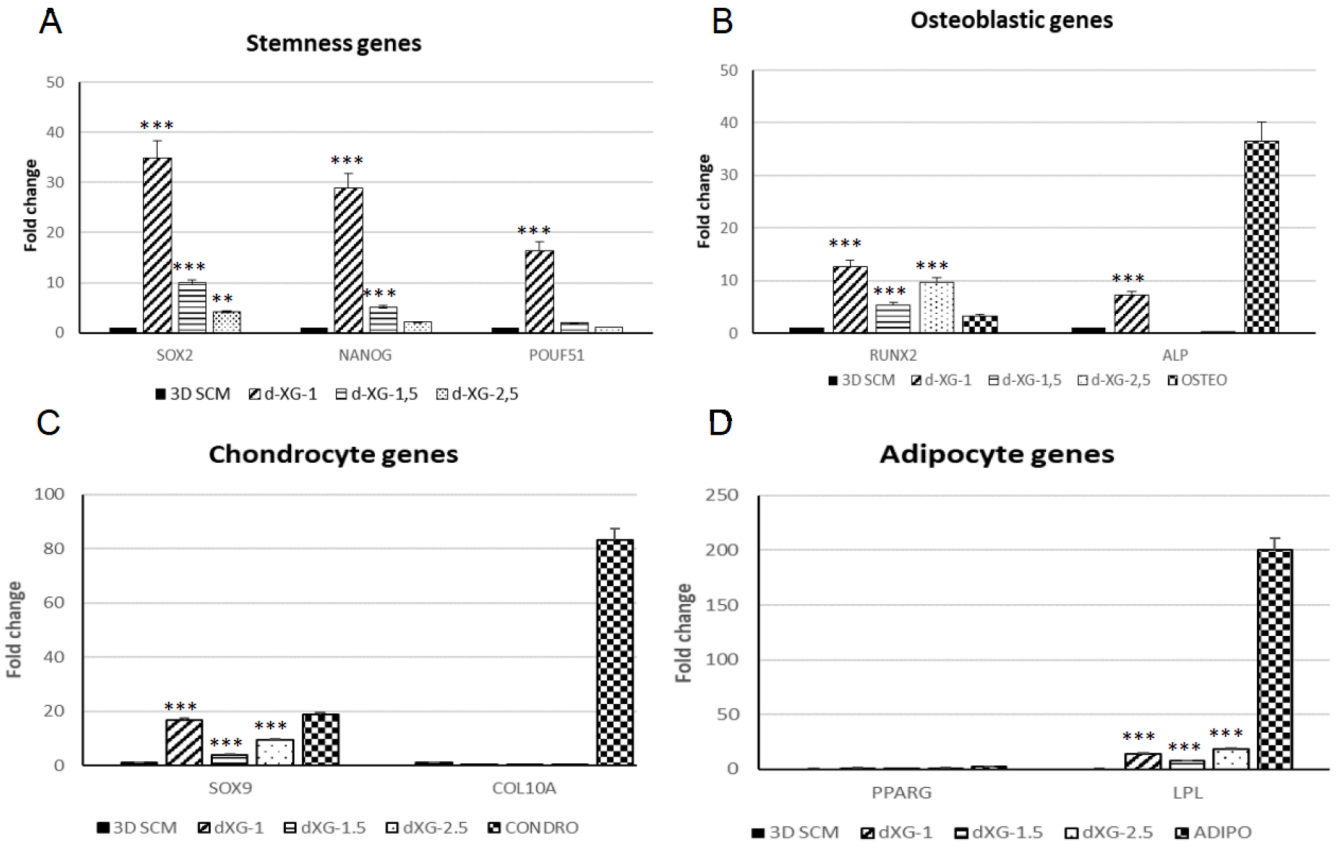

Fig. 8. Gene expression of SASCs on dXG-1, dXG-1.5 and dXG-2.5 in stemness (A), osteoblastic (B), chondrocytic (C) and adipocytic (D) conditions.

20-fold upregulated in fully differentiated fluctuating SASCs. This gene searched on SASCs-3D cells in dXG-D hydrogels gave values that were all 5-fold upregulated (Toia et al., 2020). Contrariwise, COL10A1 mRNA is downregulated in all dXG systems with DMEM, as well as in the fully differentiated scaffold-free SASCs at T21. The only cells where COL10A1 was slightly upregulated were those incorporated in dXG1-C (1.2-fold) (Fig. 8**C**).

The analysis of adipocyte characteristic genes included the nuclear transcription factor peroxisome proliferator-activated receptor γ (PPAR-γ) that plays a vital role in modulating mesenchymal lineage allocation within the bone marrow compartment, stimulating adipocyte development at the expense of osteoblast differentiation and lipoprotein lipase (LPL), that is induced in adipocyte development, The values for PPAR-g are comparable or lower than for the control and lower than that of SASCs cultured in adipocyte differentiation medium without scaffold. Contrarywise, SASCs-3D in dXG hydrogels with DMEM express higher LPL expression levels than in the control, with nearly 15-fold increase for dXG1, 8-fold increase for dXG1.5 and nearly 20-fold increase for dXG2.5 (Fig. 7**D**).

4. Discussion

Previous studies have found that partially degalactosylated xyloglucan dispersions forms biocompatible and slowly erodible gels with increasing temperature from 0–4 °C to body temperature. Both the time to gel and gel strength depend on the polymer concentration and presence of other solutes. For 2–3 %w of dXG in water the sol-to-gel transition occurs in maximum 30 min of incubation at 37 °C, yielding to relatively strong gels (G' is one order of magnitude higher than G" and frequency invariant) (Dispenza et al., 2017). At lower polymer concentration the transition is slower, and the gel is soft (at 1 %w G' is higher than G" but strongly frequency-dependent)(Todaro et al., 2015). Gelation is the result of molecular rearrangements and condensation of polymeric segments into compact domains, driven by hydrophobic interactions and balanced by repulsive hydration forces due to the presence of α-(1, 6)-D-xylose and residual β-(1, 2)-D-galactoxylose branches. These branches provide XG with high flexibility, compared to other D-glucose backbone polymers, and water solubility. Their partial removal reduces the affinity of the polymer to water, when increasing the temperature, and creates an instability region in the phase diagram of the polymer (Todaro, 2014). The macroscopic phase separation, that would occur above 20 °C, is "pinned" by gelation, which is the result of the spinodal phase separation process that leads to the formation of a network of polymer-rich regions and polymer-poor microphase domains. In this framework, it is easy to understand that the presence of salts and growth factors may have an influence on the gelation process. The mechanical spectra of dXG1-S show a G"-G' crossover at higher frequencies, dXG1-D does not (Fig. 2). The spinodal phase-separation process does not stop with macroscopic gelation, provided that the chains have the possibility to rearrange and diffuse. In conclusion, such hydrogels that form because of a local increase in polymer concentration at body temperature, and do not require the "reactive" encounter of functional groups, can tolerate better the presence of large objects, such as stem cell spheroids, and can entrap in their walls more hydrophobic solutes, such as proteins and growth factors, concentrate in the solvent rich microphase domains ions and hydrophilic solutes. Beside the ease of preparation and convenient sol-to-gel transition temperature, we were intrigued by some functional properties of xyloglucan, in virtue to its galactose branches. The review of Cho et al. (2006), Seo et al. (2005) underlines the ability of galactose-functionalised polymers to bind hepatocytes through a galactose-receptor mediated mechanism. In particular, Seog-Jin Seo et al. report a very rate of hepatocytes adhesion on xyloglucan-coated polystyrene, higher than on collagen type-I coated polystyrene (89.1 %) and on uncoated PS (25.5 %)(Seo et al., 2004). Moreover, several studies highlight the role of galectins, proteins with a high affinity for β galactose-containing oligosaccharides, secreted by several cells in promoting re-epithelialization of corneal, intestinal and skin wounds (galectin-3), corneal, skin, kidney and uterine wounds (galectin 7), and intestinal wounds (galectins-2 and -4). At the basis of re-epitalization there is cell migration (Cao et al., 2015; Panjwani, 2014) and β-galactoside-binding proteins seem to be involved in the formation of lamellipodia and activation of focal adhesion kinase in various epithelial cells. For all these reasons we considered dXG hydrogels as ideal candidates to improve SASCs viability and engrafting in regenerative medicine interventions.

Furthermore, the relationship between the porous architecture of the dXG hydrogels and cell viability can be inferred from both the SEM images (Fig. 4) and the cell viability data (Fig. 6), illustrating the influence of hydrogel microstructure on cell behavior. Hydrogels formulated with DMEM tend to form more fibrous, open, and interconnected porous networks, particularly at lower dXG concentrations (e.g., dXG1-D). This open architecture appears to facilitate nutrient and oxygen diffusion, promoting significant increases in cell viability at early time points (e.g., 1200 % at T14 for dXG1-D). In contrast, hydrogels formulated with SCM display a denser, membrane-like morphology, which corresponds to a more restrained proliferation rate, particularly in lower-concentration hydrogels like dXG1-S. Here, cell viability peak is lower (390 % at T14) and still decreases by T21 (110 %), suggesting that the compact structure and potentially distinct biochemical interactions of SCM influence both short-term proliferation and long-term viability. At higher concentrations, such as dXG2.5, the porous architecture becomes more compact and uniform across both media. Interestingly, these dense structures may restrict cell proliferation, compared to more open systems. For instance, dXG2.5-S in SCM achieves medium-high viability (500 % at T14) that goes down at T21 (230 %). The porous architecture, modulated by polymer concentration and culture medium, not only influences nutrient transport but also provides varying degrees of mechanical and biochemical cues to cells. The different cell behavior observed can be due to the distinct tendencies of cells within scaffolds prepared using the two different media. With SCM, SASCs are continuously stimulated to remain stem cells. In contrast, without induction to maintain the stem cell state, the scaffold interaction drives cells to spread and even differentiate. This spreading is possible in dXG1, which has an open structure, but becomes more challenging as polymer concentration increases, reducing porosity.

For what concerns the discussion on cell viability, we investigated dXG1 with SASCs in stemness conditions first to find out that they 100 % viable after 1, 7 and 21 days of incubation. Not having taken the point after 14 days, we missed the 5-fold increase in cell viability at T14 that we have seen now (Fig. 6**A**). At T21, SASCs embedded in dXG1 showed upregulation of stemness genes (SOX2, NANOG and POUF1) compared with scaffold-free SASCs cultured with the same medium (Muscolino et al., 2021). The stemness-related genes (SOX2, NANOG, and POUF1) are transcription factors that play important roles in maintaining the pluripotent state of embryonic stem cells(Boyer et al., 2005). These genes have been found to be expressed in various stem cell types, including Bone Marrow Mesenchymal Stem Cells (BM-MSCs) and Adipose-derived Stem Cells (ASCs) (Tsai & Hung, 2012). The upregulation of these genes with respect to free spheroids is even more significant, considering that these genes in spheroids (SASCs-3D) are already upregulated compared to traditional 2D cell culture (ASCs-2D). This suggests that dXG hydrogels provide a more favourable environment for the maintenance of SASCs structure and features. In another study, we examined the behaviour of SASCs-laden dXG hydrogels in chondrogenic and osteoblastic differentiation conditions. CDM and ODM were added to the formulation and in small quantities also during the incubation. The results indicated that SASCs-laden dXG hydrogels, after the first week where a selection seems to occur in some conditions, showed higher proliferation rates than free SASCs, incubated with CDM or ODM. The cell viability was highest in dXG1-C after 21 days. More in general, at T21 cell viability values in CDM were the highest also for dXG1.5 and dXG2.5, if compared with the analogous systems formulated

with SCM or ODM (Fig. 7). The differentiation with both media occurred only toward the target lineage, supporting the important role of the scaffold and the biochemical cues provided with the differentiative media. Gene and protein expression analyses at T21 were used to confirm the success of differentiation. In this work we wanted to understand if dXG has also active role in supporting cell proliferation and differentiation. To this aim, we used DMEM as growth medium because is devoid of specific biomolecules that stimulate differentiation. We measured cell viability and searched for various genes that are associated to stemness showing that hydrogels stimulate SASCs to proliferate and maintaining stemness properties. The peak in cell viability for gels formulated with DMEM was at T14 irrespective of polymer concentration. We observed that stemness-associated genes are highly upregulated for SASCs incorporated in dXG1 and continue to be upregulated but less as polymer concentration increases. Probably the downregulation of stemness genes to the increase of concentrations of dXG could be due to the initial expression of differentiative genes, as RUNX2 and SOX9. In fact, in dXG2.5 the expression of RUNX2 and SOX9 increased. All the genes associated with early stages of differentiation are also highly upregulated for SASCs in dXG, especially if compared to those in cells that have reached full differentiation. For all systems, their values have a minimum for the intermediate polymer concentration. Regarding the genes related to more mature stages of differentiation, ALP in dXG1 and LPL in all systems, were the only ones expressed.

We can imagine that most spheroids in dXG1 have retained their structure, initially housed in larger cavities in which metabolites are concentrated, and properly spaced. Their stemness is enhanced. Isolated cells and those in the spheroids that get in contact with the hydrogel pore walls can also find an ideal support for their adhesion, spreading, and proliferation. Their expansion leads to the development of genes characteristic of their differentiation into the typical lineages of differentiated MSC, with a higher commitment toward chondrocytic and adipocytic differentiation. When the polymer concentration increases, the viscosity in the pre-gel phase increases and the gelation time decreases. Spheroids that were disaggregated for cell counting have no longer the possibility to cluster. In dXG2.5 stemness genes decrease as a consequence of the cell-polymer interaction that promotes their adhesion and migration (spreading). While stemness decreases, the differentiation process begins (with a more pronounced toward the adipose lineage).

Several studies, in agreement with our data, have demonstrated that biochemical, physical, and mechanical stimuli can modulate stem cell fate and the expression of stemness-related genes. Changes in the physico-chemical environment can regulate gene expression, thereby influencing stem cell behavior.

To date, there are no studies in the literature specifically addressing xyloglucan or its degalactosylated variant in this context. However, findings with other hydrogels provide valuable parallels. For instance, Choi et al. (2016) demonstrated that the crosslinking degree and hence the stiffness of polyacrylamide hydrogels (ranging from 0.1 to 20 kPa) can direct cell fate and reprogram mouse embryonic fibroblasts into induced pluripotent stem cells (iPSCs) through activation of the mesenchymal-to-epithelial transition. Notably, they observed enhanced expression of stemness markers, such as OCT4 and SOX2, on softer substrates (0.1 kPa) compared to stiffer ones (20 kPa). Similar effects of soft substrates on the maintenance of stemness and stemness marker expression have been reported by other groups (Chowdhury et al., 2010; Higuchi et al., 2014; Lü et al., 2014), highlighting that this phenomenon occurs through the downregulation of cell-matrix traction forces. Studies on hydrogels based on alginate with hyaluronic acid (Pangjantuk et al., 2024), or gelatin (Li et al., 2021) similarly showed a significant upregulation of stemness such as SOX2, NANOG, and OCT4and proliferation genes as Ki67.

Additionally, McMurray et al. (2011) demonstrated that nanostructured surfaces can maintain mesenchymal stem cell (MSC) phenotype and multipotency by inducing a quiescent state, which prevents differentiation. Similarly, Gilbert et al., (2010) showed that muscle stem cells cultured on soft hydrogels mimicking their natural microenvironment avoided differentiation by preventing the activation of key signaling pathways.

In our study, the microenvironment created by dXG, particularly at the 1 %w concentration, significantly supports the expression of stemness genes. The correlation between extracellular matrix composition and stem cell gene regulation underscores the importance of further investigating these interactions to optimize the application of dXG and similar materials in clinical settings. The increased rigidity of the scaffold probably provides mechanical signals that "push" the stem cells to embark on a differentiative pathway. On the other hand, the study of the effect of dXG concentration on the proliferation rate of SASCs showed a distinct trend at each different experimental point with different culture media. Our focus then became to understand whether a specific condition (concentrations of dXG and/or SASCs mesenchymal differentiative abilities) could be used in a specific regenerative field. In particular, the highest proliferation peaks at 21 days in CDM: 10 fold in dXG1, ~3 fold in dXG1.5 and 4 fold in dXG2.5, would lead us to say that SASCs incorporated with dXG might be a good solution for cartilage regeneration. dXG1 could be an injectable solution, while dXG2.5 could be also implantable directly on the lesion or defect. In a bone context, SASCs could be an injected together with dXG1, showing an increase of viability of 3 fold. Instead, in a condition in which is necessary to have a great amount of cells, with stemness properties, you would have to choose a generic condition in DMEM and in dXG1.

5. Conclusions

Partially degalactosylated xyloglucan gels are very interesting niches for adipose stem cells for their ability of support their viability and differentiation potential, even when formulated and incubated with specific factors. At all concentrations investigated, but especially at low concentration, dXG gels swollen by DMEM they enhance stem cells stemness. The inverse relation of the expression of stemness genes with polymer concentration of the hydrogel can be attributed to the looser and more conformable polymer network formed at low concentration, that can allow ASC reassembly in spheroids after incorporation in the gel. They can also support stem cells expansion and development of early genes that are characteristic of their differentiation into the typical lineages of differentiated MSC, with a higher commitment toward chondrocytic and adipocytic differentiation. In conclusion, the simplest system, containing only dXG at the lowest concentration (1 %w) and no biochemical stimulation, resulted the best scaffold to support cell proliferation and predispose SASCs towards mesenchymal differentiation. Hence, dXG1 is the most interesting for further in vivo evaluation in the context of chondro-articular lesion treatment.

Funding sources

Clelia Dispenza, Anna Barbara Di Stefano and Adriana Cordova were funded by the "Sicilian MicronanoTech Research And Innovation Center" - SAMOTHRACE – (B73C22000810001 - ECS_00000022) Spoke 3, and by "Piano strategico per il miglioramento della qualità della ricerca e dei risultati della VQR-Misura B" - PJ_UTILE_2022_VQR. Emanuela Muscolino has received funding from the European Union - NextGenerationEU through the Italian Ministry of University and Research under PNRR - M4C2-I1.3 Project PE_00000019 "HEAL ITALIA" CUP B73C22001250006. The views and opinions expressed are those of the authors only and do not necessarily reflect those of the European Union or the European Commission. Neither the European Union nor the European Commission can be held responsible for them.

CRediT authorship contribution statement

Anna Barbara Di Stefano: Writing – original draft, Visualization,

Validation, Project administration, Methodology, Investigation, Data curation, Conceptualization. **Emanuela Muscolino:** Writing – original draft, Visualization, Validation, Project administration, Methodology, Investigation, Data curation, Conceptualization. **Marco Trapani:** Investigation, Data curation. **Francesco Moschella:** Supervision. **Bartolo Corradino:** Supervision. **Francesca Toia:** Supervision. **Adriana Cordova:** Supervision, Resources, Funding acquisition. **Clelia Dispenza:** Writing – review & editing, Supervision, Resources, Funding acquisition.

Declaration of competing interest

The authors declare that they have no known competing financial interests or personal relationships that could have appeared to influence the work reported in this paper.

Acknowledgements

We wish to acknowledge Dr. Daniela Giacomazza of Istituto di Biofisica, Consiglio Nazionale delle Ricerche, Via U. La Malfa 153, 90146 Palermo, Italy, for support during the rheological experiments.

Data availability

Data will be made available on request.

References

Bertsch, P., Andrée, L., Besheli, N. H., & Leeuwenburgh, S. C. G. (2022). Colloidal hydrogels made of gelatin nanoparticles exhibit fast stress relaxation at strains relevant for cell activity. *Acta Biomaterialia, 138*, 124–132. https://doi.org/10.1016/j.actbio.2021.10.053

Boyer, L. A., Lee, T. I., Cole, M. F., Johnstone, S. E., Levine, S. S., Zucker, J. P., Guenther, M. G., Kumar, R. M., Murray, H. L., Jenner, R. G., Gifford, D. K., Melton, D. A., Jaenisch, R., & Young, R. A. (2005). Core transcriptional regulatory circuitry in human embryonic stem cells. *Cell, 122*(6), 947–956. https://doi.org/10.1016/j.cell.2005.08.020

Brun-Graeppi, A. K. A. S., Richard, C., Bessodes, M., Scherman, D., Narita, T., Ducouret, G., & Merten, O.-W. (2010). Study on the sol–gel transition of xyloglucan hydrogels. *Carbohydrate Polymers, 80*(2), 555–562. https://doi.org/10.1016/j.carbpol.2009.12.026

Cameron, A. R., Frith, J. E., Gomez, G. A., Yap, A. S., & Cooper-White, J. J. (2014). The effect of time-dependent deformation of viscoelastic hydrogels on myogenic induction and Rac1 activity in mesenchymal stem cells. *Biomaterials, 35*(6), 1857–1868. https://doi.org/10.1016/j.biomaterials.2013.11.023

Cameron, Andrew. R., Frith, Jessica. E., & Cooper-White, Justin. J. (2011). The influence of substrate creep on mesenchymal stem cell behaviour and phenotype. *Biomaterials, 32*(26), 5979–5993. https://doi.org/10.1016/j.biomaterials.2011.04.003

Cao, Z., Saravanan, C., Chen, W.-S., & Panjwani, N. (2015). Examination of the role of galectins in cell migration and *Re*-epithelialization of wounds. In S. R. Stowell, & R. D. Cummings (Eds.), *Galectins* (pp. 317–326). New York: Springer. https://doi.org/10.1007/978-1-4939-1396-1_21, 1207.

Chen, D., Guo, P., Chen, S., Cao, Y., Ji, W., Lei, X., Liu, L., Zhao, P., Wang, R., Qi, C., Liu, Y., & He, H. (2012). Properties of xyloglucan hydrogel as the biomedical sustained-release carriers. *Journal of Materials Science: Materials in Medicine, 23*(4), 955–962. https://doi.org/10.1007/s10856-012-4564-z

Cho, C. S., Seo, S. J., Park, I. K., Kim, S. H., Kim, T. H., Hoshiba, T., Harada, I., & Akaike, T. (2006). Galactose-carrying polymers as extracellular matrices for liver tissue engineering. *Biomaterials, 27*(4), 576–585. https://doi.org/10.1016/j.biomaterials.2005.06.008

Choi, B., Park, K., Kim, J., Ko, K., Kim, J., Han, D. K., & Lee, S. (2016). Stiffness of hydrogels regulates cellular reprogramming efficiency through mesenchymal-to-epithelial transition and stemness markers. *Macromolecular Bioscience, 16*(2), 199–206. https://doi.org/10.1002/mabi.201500273

Chowdhury, F., Li, Y., Poh, Y.-C., Yokohama-Tamaki, T., Wang, N., & Tanaka, T. S. (2010). Soft substrates promote homogeneous self-renewal of embryonic stem cells via downregulating cell-matrix tractions. *PLoS ONE, 5*(12), e15655. https://doi.org/10.1371/journal.pone.0015655

Cosson, S., Otte, E. A., Hezaveh, H., & Cooper-White, J. J. (2015). Concise review: Tailoring bioengineered scaffolds for stem cell applications in tissue engineering and regenerative medicine. *Stem Cells Translational Medicine, 4*(2), 156–164. https://doi.org/10.5966/sctm.2014-0203

De Freitas, R. A., Busato, A. P., Mitchell, D. A., & Silveira, J. L. M. (2011). Degalatosylation of xyloglucan: Effect on aggregation and conformation, as determined by time dependent static light scattering, HPSEC–MALLS and viscosimetry. *Carbohydrate Polymers, 83*(4), 1636–1642. https://doi.org/10.1016/j.carbpol.2010.10.021

Dea, I. C. M. (1989). Industrial polysaccharides. *Pure and Applied Chemistry, 61*(7), 1315–1322. https://doi.org/10.1351/pac198961071315

Di Stefano, A. B., Grisafi, F., Perez-Alea, M., Castiglia, M., Di Simone, M., Meraviglia, S., Cordova, A., Moschella, F., & Toia, F. (2021a). Cell quality evaluation with gene expression analysis of spheroids (3D) and adherent (2D) adipose stem cells. *Gene, 768*, Article 145269. https://doi.org/10.1016/j.gene.2020.145269

Di Stefano, A. B., Leto Barone, A. A., Giammona, A., Apuzzo, T., Moschella, P., Di Franco, S., Giunta, G., Carmisciano, M., Eleuteri, C., Todaro, M., Dieli, F., Cordova, A., Stassi, G., & Moschella, F. (2016). Identification and expansion of adipose stem cells with enhanced bone regeneration properties. *Journal of Regenerative Medicine, 05*(01). https://doi.org/10.4172/2325-9620.1000124

Di Stefano, A. B., Montesano, L., Belmonte, B., Gulino, A., Gagliardo, C., Florena, A. M., Bilello, G., Moschella, F., Cordova, A., Leto Barone, A. A., & Toia, F. (2021b). Human spheroids from adipose-derived stem cells induce calvarial bone production in a xenogeneic rabbit model. *Annals of Plastic Surgery, 86*(6), 714–720. https://doi.org/10.1097/SAP.0000000000002579

Dispenza, C., Todaro, S., Bulone, D., Sabatino, M. A., Ghersi, G., San Biagio, P. L., & Lo Presti, C. (2017). Physico-chemical and mechanical characterization of in-situ forming xyloglucan gels incorporating a growth factor to promote cartilage reconstruction. *Materials Science and Engineering: C, 70*, 745–752. https://doi.org/10.1016/j.msec.2016.09.045

Dispenza, C., Todaro, S., Sabatino, M. A., Chillura Martino, D., Martorana, V., San Biagio, P. L., Maffei, P., & Bulone, D. (2020). Multi-scale structural analysis of xyloglucan colloidal dispersions and hydro-alcoholic gels. *Cellulose, 27*(6), 3025–3035. https://doi.org/10.1007/s10570-020-03004-0

Engler, A. J., Sen, S., Sweeney, H. L., & Discher, D. E. (2006). Matrix elasticity directs stem cell lineage specification. *Cell, 126*(4), 677–689. https://doi.org/10.1016/j.cell.2006.06.044

Fry, S. C. (1988). *The growing plant cell wall: chemical and metabolic analysis (1. publ).* Longman Scientific & Technical.

Gilbert, P. M., Havenstrite, K. L., Magnusson, K. E. G., Sacco, A., Leonardi, N. A., Kraft, P., Nguyen, N. K., Thrun, S., Lutolf, M. P., & Blau, H. M. (2010). Substrate elasticity regulates skeletal muscle stem cell self-renewal in culture. *Science, 329*(5995), 1078–1081. https://doi.org/10.1126/science.1191035

Gimble, J. M., Katz, A. J., & Bunnell, B. A. (2007). Adipose-derived stem cells for regenerative medicine. *Circulation Research, 100*(9), 1249–1260. https://doi.org/10.1161/01.RES.0000265074.83288.09

Federica, Gulino, Emanuela, Muscolino, Sabina, Alessi, Domenico, Nuzzo, Pasquale, Picone, Daniela, Giacomazza, & Clelia, Dispenza (2024). Hydrogel dressings with egg white proteins for wound healing. *Chemical Engineering Transactions, 110*, 247–252. https://doi.org/10.3303/CET24110042

Han, Y., Li, X., Zhang, Y., Han, Y., Chang, F., & Ding, J. (2019). Mesenchymal stem cells for regenerative medicine. *Cells, 8*(8), 886. https://doi.org/10.3390/cells8080886

Higuchi, S., Watanabe, T. M., Kawauchi, K., Ichimura, T., & Fujita, H. (2014). Culturing of mouse and human cells on soft substrates promote the expression of stem cell markers. *Journal of Bioscience and Bioengineering, 117*(6), 749–755. https://doi.org/10.1016/j.jbiosc.2013.11.011

Ilie, I., Ilie, R., Mocan, T., Bartos, D., & Mocan, L. (2012). Influence of nanomaterials on stem cell differentiation: Designing an appropriate nanobiointerface. *International Journal of Nanomedicine, 7*, 2211–2225. https://doi.org/10.2147/IJN.S29975

Joon Kwon, H. (2013). Chondrogenesis on sulfonate-coated hydrogels is regulated by their mechanical properties. *Journal of the Mechanical Behavior of Biomedical Materials, 17*, 337–346. https://doi.org/10.1016/j.jmbbm.2012.10.006

Kawasaki, N., Ohkura, R., Miyazaki, S., Uno, Y., Sugimoto, S., & Attwood, D. (1999). Thermally reversible xyloglucan gels as vehicles for oral drug delivery. *International Journal of Pharmaceutics, 181*(2), 227–234. https://doi.org/10.1016/S0378-5173(99)00026-5

Li, J., Zhang, Y., Enhe, J., Yao, B., Wang, Y., Zhu, D., Li, Z., Song, W., Duan, X., Yuan, X., Fu, X., & Huang, S. (2021). Bioactive nanoparticle reinforced alginate/gelatin bioink for the maintenance of stem cell stemness. *Materials Science and Engineering: C, 126*, Article 112193. https://doi.org/10.1016/j.msec.2021.112193

Lü, D., Luo, C., Zhang, C., Li, Z., & Long, M. (2014). Differential regulation of morphology and stemness of mouse embryonic stem cells by substrate stiffness and topography. *Biomaterials, 35*(13), 3945–3955. https://doi.org/10.1016/j.biomaterials.2014.01.066

Mahajan, H. S., & Mahajan, P. R. (2016). Development of grafted xyloglucan micelles for pulmonary delivery of curcumin: In vitro and in vivo studies. *International Journal of Biological Macromolecules, 82*, 621–627. https://doi.org/10.1016/j.ijbiomac.2015.09.053

McMurray, R. J., Gadegaard, N., Tsimbouri, P. M., Burgess, K. V., McNamara, L. E., Tare, R., Murawski, K., Kingham, E., Oreffo, R. O. C., & Dalby, M. J. (2011). Nanoscale surfaces for the long-term maintenance of mesenchymal stem cell phenotype and multipotency. *Nature Materials, 10*(8), 637–644. https://doi.org/10.1038/nmat3058

Miyazaki, S., Kawasaki, N., Kubo, W., Endo, K., & Attwood, D. (2001a). Comparison of in situ gelling formulations for the oral delivery of cimetidine. *International Journal of Pharmaceutics, 220*(1–2), 161–168. https://doi.org/10.1016/S0378-5173(01)00669-X

Miyazaki, S., Suisha, F., Kawasaki, N., Shirakawa, M., Yamatoya, K., & Attwood, D. (1998). Thermally reversible xyloglucan gels as vehicles for rectal drug delivery. *Journal of Controlled Release, 56*(1–3), 75–83. https://doi.org/10.1016/S0168-3659(98)00079-0

Miyazaki, S., Suzuki, S., Kawasaki, N., Endo, K., Takahashi, A., & Attwood, D. (2001b). In situ gelling xyloglucan formulations for sustained release ocular delivery of pilocarpine hydrochloride. *International Journal of Pharmaceutics, 229*(1–2), 29–36. https://doi.org/10.1016/S0378-5173(01)00825-0

Muscolino, E., Di Stefano, A. B., Toia, F., Giacomazza, D., Moschella, F., Cordova, A., & Dispenza, C. (2024). Xyloglucan, alginate and k-carrageenan hydrogels on spheroids of adipose stem cells survival; preparation, mechanical characterization, morphological analysis and injectability. *Carbohydrate Polymer Technologies and Applications, 8*, Article 100566. https://doi.org/10.1016/j.carpta.2024.100566

Muscolino, E., Di Stefano, A. B., Trapani, M., Sabatino, M. A., Giacomazza, D., Moschella, F., Cordova, A., Toia, F., & Dispenza, C. (2021). Injectable xyloglucan hydrogels incorporating spheroids of adipose stem cells for bone and cartilage regeneration. *Materials Science and Engineering: C, 131*, Article 112545. https://doi.org/10.1016/j.msec.2021.112545

Muscolino, E., Sabatino, M. A., Jonsson, M., & Dispenza, C. (2024). The role of water in radiation-induced fragmentation of cellulosic backbone polysaccharides. *Cellulose, 31*(2), 841–856. https://doi.org/10.1007/s10570-023-05660-4

Nisbet, D. R., Crompton, K. E., Hamilton, S. D., Shirakawa, S., Prankerd, R. J., Finkelstein, D. I., Horne, M. K., & Forsythe, J. S. (2006). Morphology and gelation of thermosensitive xyloglucan hydrogels. *Biophysical Chemistry, 121*(1), 14–20. https://doi.org/10.1016/j.bpc.2005.12.005

Pangjantuk, A., Kaokaen, P., Kunhorm, P., Chaicharoenaudomrung, N., & Noisa, P. (2024). 3D culture of alginate-hyaluronic acid hydrogel supports the stemness of human mesenchymal stem cells. *Scientific Reports, 14*(1), 4436. https://doi.org/10.1038/s41598-024-54912-1

Panjwani, N. (2014). Role of galectins in re-epithelialization of wounds. *Annals of Translational Medicine, 2*(9), 89. https://doi.org/10.3978/j.issn.2305-5839.2014.09.09

Picone, P., Muscolino, E., Girgenti, A., Testa, M., Giacomazza, D., Dispenza, C., & Nuzzo, D. (2024). Mitochondria embedded in degalactosylated xyloglucan hydrogels to improve mitochondrial transplantation. *Carbohydrate Polymer Technologies and Applications, 8*, Article 100543. https://doi.org/10.1016/j.carpta.2024.100543

Seib, F. P., Prewitz, M., Werner, C., & Bornhäuser, M. (2009). Matrix elasticity regulates the secretory profile of human bone marrow-derived multipotent mesenchymal stromal cells (MSCs). *Biochemical and Biophysical Research Communications, 389*(4), 663–667. https://doi.org/10.1016/j.bbrc.2009.09.051

Seo, S.-J., Akaike, T., Choi, Y.-J., Shirakawa, M., Kang, I.-K., & Cho, C.-S. (2005). Alginate microcapsules prepared with xyloglucan as a synthetic extracellular matrix for hepatocyte attachment. *Biomaterials, 26*(17), 3607–3615. https://doi.org/10.1016/j.biomaterials.2004.09.025

Seo, S.-J., Park, I.-K., Yoo, M.-K., Shirakawa, M., Akaike, T., & Cho, C.-S. (2004). Xyloglucan as a synthetic extracellular matrix for hepatocyte attachment. *Journal of Biomaterials Science, Polymer Edition, 15*(11), 1375–1387. https://doi.org/10.1163/1568562042368059

Shirakawa, M., Yamatoya, K., & Nishinari, K. (1998). Tailoring of xyloglucan properties using an enzyme. *Food Hydrocolloids, 12*(1), 25–28. https://doi.org/10.1016/S0268-005X(98)00052-6

Takahashi, A., Suzuki, S., Kawasaki, N., Kubo, W., Miyazaki, S., Loebenberg, R., Bachynsky, J., & Attwood, D. (2002). Percutaneous absorption of non-steroidal anti-inflammatory drugs from in situ gelling xyloglucan formulations in rats. *International Journal of Pharmaceutics, 246*(1–2), 179–186. https://doi.org/10.1016/S0378-5173(02)00394-0

Todaro, S. (2014). *Xyloglucan self-assembled nanostructures and gels for biomedical applications*. Università degli Studi di Palermo. https://iris.unipa.it/retrieve/handle/10447/108717/152942/TODARO_PhD%20Dissertation.pdf.

Todaro, S., Dispenza, C., Sabatino, M. A., Ortore, M. G., Passantino, R., San Biagio, P. L., & Bulone, D. (2015). Temperature-induced self-assembly of degalactosylated xyloglucan at low concentration. *Journal of Polymer Science Part B: Polymer Physics, 53*(24), 1727–1735. https://doi.org/10.1002/polb.23895

Toia, F., Di Stefano, A. B., Muscolino, E., Sabatino, M. A., Giacomazza, D., Moschella, F., Cordova, A., & Dispenza, C. (2020). In-situ gelling xyloglucan formulations as 3D artificial niche for adipose stem cell spheroids. *International Journal of Biological Macromolecules, 165*, 2886–2899. https://doi.org/10.1016/j.ijbiomac.2020.10.158

Tsai, C.-C., & Hung, S.-C. (2012). Functional roles of pluripotency transcription factors in mesenchymal stem cells. *Cell Cycle (Georgetown, Tex.), 11*(20), 3711–3712. https://doi.org/10.4161/cc.22048

Zhang, E., Li, J., Zhou, Y., Che, P., Ren, B., Qin, Z., Ma, L., Cui, J., Sun, H., & Yao, F. (2017). Biodegradable and injectable thermoreversible xyloglucan based hydrogel for prevention of postoperative adhesion. *Acta Biomaterialia, 55*, 420–433. https://doi.org/10.1016/j.actbio.2017.04.003